RESEARCH ARTICLE

PrP-containing aggresomes are cytosolic components of an ER quality control mechanism

Tatyana Dubnikov[1], Tziona Ben-Gedalya[1,2], Robert Reiner[1], Dominic Hoepfner[3], Wayne A. Cabral[4], Joan C. Marini[4] and Ehud Cohen[1,*]

ABSTRACT

Limited detoxification capacity often directs aggregation-prone, potentially hazardous, misfolded proteins to be deposited in designated cytosolic compartments known as 'aggresomes'. The roles of aggresomes as cellular quality control centers, and the cellular origin of the deposits contained within these structures, remain to be characterized. Here, we utilized the observation that the prion protein (PrP, also known as PRNP) accumulates in aggresomes following the inhibition of folding chaperones, members of the cyclophilin family, to address these questions. We found that misfolded PrP molecules must pass through the endoplasmic reticulum (ER) in order to be deposited in aggresomes, that the Golgi plays no role in this process and that cytosolic PrP species are not deposited in pre-existing aggresomes. Prior to their deposition in the aggresome, PrP molecules lose the ER localization signal and have to acquire a GPI anchor. Our discoveries indicate that PrP aggresomes are cytosolic overflow deposition centers for the ER quality control mechanisms and highlight the importance of these structures for the maintenance of protein homeostasis within the ER.

KEY WORDS: Protein aggregation, Aggresome, Prion protein, Endoplasmic reticulum, Neurodegeneration

INTRODUCTION

The maturation of newly synthesized polypeptides is a multi-step process that is assisted and supervised by a network of molecular chaperones (Kim et al., 2013). Unlike cytosolic proteins, secreted and membrane proteins bear N-terminal signal peptides that mediate their co-translational insertion into the endoplasmic reticulum (ER), an intracellular organelle that is specialized in protein folding, post-translational modification and quality control. In the ER, the polypeptide is processed by a highly ordered set of components that remove its signal peptide and promote the correct folding of the molecule (Ruggiano et al., 2014). Despite the activity of these ER-resident mechanisms, a substantial fraction of the nascent polypeptides fail to attain their desired spatial conformation (Schubert et al., 2000), retro-translocate to the cytosol and are designated for degradation by the ER-associated degradation (ERAD) machinery (Merulla et al., 2013) or by autophagy

(Suntharalingam et al., 2012). Occasionally, subsets of aggregation-prone proteins evade quality control surveillance and form potentially hazardous, insoluble aggregates. Specialized chaperones can disrupt such aggregates to enable their degradation (Duennwald et al., 2012). However, owing to a limited capacity of these disaggregation and degradation mechanisms or because of an exceptionally high propensity of certain polypeptides to aggregate, protein aggregates sometimes accumulate within the cell. To avoid protein-aggregate-associated toxicity, cells deposit aggregated proteins in specialized sites such as aggresomes (Johnston et al., 1998). Aggresomes are cytosolic structures that are formed around the microtubule-organizing center (MTOC) and confined by collapsed vimetin fibers (Johnston et al., 1998).

Uncontrolled protein aggregation underlies the development of devastating maladies that are collectively termed 'proteinopathies' (Walker et al., 2006). Neurodegenerative disorders such as Alzheimer's disease and prion disorders constitute a subgroup of proteinopathies (Selkoe, 2003). Accordingly, the deposition of insoluble protein aggregates in designated cellular or extracellular sites is a hallmark of various neurodegenerative illnesses (Soto, 2003).

The prion protein (PrP, also known as PRNP) is an aggregation-prone glycosyl-phosphatidyl-inositol (GPI)-anchored glycoprotein that is processed in the secretory pathway (Prusiner, 1998). Shortly after translocation into the ER, the N-terminal ER localization signal is cleaved and a GPI anchor is attached to the C-terminus of the protein. The GPI tail has crucial roles in the maturation of PrP in the secretory pathway and in anchoring the mature protein to cholesterol-rich lipid micro-domains of the cell surface (Naslavsky et al., 1997). The protein also undergoes N-linked glycosylation and a disulfide bridge is formed within the ER as part of its maturation process. Additional processing events, including the attachment of complex carbohydrates, occur at the Golgi complex (Taraboulos et al., 1992).

PrP is expressed in different cell types, including neurons, where its aggregation underlies the development of several late-onset degenerative disorders. Kuru, Creutzfeldt–Jakob disease (CJD), Gerstmann–Sträussler–Scheinker syndrome (GSS) and fatal familial insomnia (FFI) are terminal prion disorders that exhibit different etiologies and distinct patterns of manifestation (reviewed in Aguzzi and Calella, 2009). Although GSS and FFI manifest exclusively as mutation-linked familial disorders, CJD can emerge sporadically as a result of mutations in the sequence of PrP or due to infection (Prusiner, 1998).

Although rare, prion-disorder-linked mutations provide invaluable hints that help decipher the mechanisms that lead to the emergence of these illnesses. The substitution of leucine for proline P102 (P102L) (Hsiao et al., 1989), or of leucine or serine for proline P105 (P102L/S) (Yamazaki et al., 1999) in PrP is among the

[1]Biochemistry and Molecular Biology, the Institute for Medical Research Israel – Canada (IMRIC), the School of Medicine of the Hebrew University of Jerusalem, Jerusalem 91120, Israel. [2]Department of Obstetrics and Gynecology, Hadassah University Hospital, Ein Kerem, Jerusalem, 91120, Israel. [3]Novartis Institutes for BioMedical Research, Novartis Campus, Basel 4056, Switzerland. [4]Bone and Extracellular Matrix Branch, NICHD, NIH, Bethesda, MD 20892, USA.

*Author for correspondence (ehudc@ekmd.huji.ac.il)

E.C., 0000-0001-5552-7086

mutations that underlie the development of GSS. Previously, we have found that these mutations preclude PrP from folding properly by abolishing the recognition sites for folding chaperones, members of the cyclophilin family of proline cis-trans isomerases (Barik, 2006). Similarly, wild-type PrP misfolds and forms aggregates following treatment with the cyclophilin-specific inhibitor cyclosporin-A (CsA). CsA-induced misfolded PrP species accumulate in aggresomes (Cohen and Taraboulos, 2003), which serve as cytosolic dynamic quality control compartments that attract molecular chaperones and proteasomes (Ben-Gedalya et al., 2011). Both the prerequisites for directing misfolded PrP molecules to aggresomes and the location at which triage of these potentially hazardous species occurs remain unclear. Here, we created a series of fluorescently tagged PrP mutants and followed their fates in CsA-treated cells. Interestingly, we discovered that PrP molecules must enter the ER in order to be directed to aggresomes. However, cytosolic PrP molecules did not reach pre-existing aggresomes. The attachment of a GPI moiety to PrP and the glycosylation of residue 180, but not residue 196, of the protein were also prerequisites for the deposition of these molecules in the aggresome. In contrast, the Golgi had no role in directing PrP to these structures. Our observations indicate that cytosolic aggresomes are tightly associated with the ER quality control mechanism and highlight the importance of the ER for the maintenance of cellular protein homeostasis (proteostasis) (Balch et al., 2008).

Results

Aggresome-resident CsA-induced misfolded PrP molecules originate solely from the ER

Owing to the limited efficiency of the N-terminal ER-localization signal of PrP (Rane et al., 2010), two subpopulations of PrP molecules exist within cells that overexpress PrP. One subpopulation stays in the cytosol whereas the other consists of PrP molecules that enter the ER and are processed through the secretory pathway. PrP molecules that mature properly are eventually presented on the cell surface, whereas their cytosolic counterparts are directed for degradation by the ubiquitin proteasome system (UPS) (Drisaldi et al., 2003; Yedidia et al., 2001). To test whether aggresome-resident PrP species originate from the cytosol, the ER or from both compartments, we created fluorescently tagged PrP molecules that either efficiently entered the ER or remained entirely cytosolic. To achieve this, we used the MHM_2 PrP chimera (Scott et al., 1992) labeled with yellow fluorescent protein (wt SP-YFP-PrP) (Ben-Gedalya et al., 2011) and replaced the natural PrP ER-localization signal with that of the bovine hormone prolactin (Prl SP-YFP-PrP) or of the rat osteopontin (Opn SP-YFP-PrP) (Fig. 1A). Both signal peptides were shown to efficiently mediate the entry of PrP into ER-like vesicles in an in vitro system (Kim et al., 2002) (for the ER signal amino acid sequences, see Fig. S1A). To obtain an entirely cytosolic PrP population, we removed the DNA sequence that encodes the ER localization signal (ΔSP YFP-PrP) (Fig. 1A). The constructs were transfected into Chinese hamster ovary (CHO) cells and stable lines were isolated. Western blot analysis revealed that cells transfected with either Opn SP-YFP-PrP (Fig. 1B, lane 3) or Prl SP-YFP-PrP (lane 4) expressed moderate quantities of PrP; less than cells that expressed the wt SP-YFP-PrP construct (lane 2). Deglycosylation by the enzyme N-glycosidase F (PNGase F) and western blot analysis confirmed that the wt SP-YFP-PrP and Opn SP-YFP-PrP underwent glycosylation (Fig. S1B), indicating that these molecules enter the ER. Similarly, we used PNGase F to examine whether Opn SP-RFP-PrP was glycosylated and found that the attachment of a red

fluorescent protein (RFP) to this PrP construct did not prevent it from entering the ER (Fig. S1C).

The relatively low amounts of ΔSP YFP-PrP that were observed in the cells (Fig. 1B, lane 5) suggested that YFP–PrP molecules that failed to enter the ER underwent proteasome-mediated degradation (Drisaldi et al., 2003). To test this and further confirm the efficiency of the Prl and Opn ER localization signals, we transfected naïve CHO cells with non-fluorescently-tagged PrP constructs that either bear the wt PrP, Prl or Opn ER localization signal or lacked such a signal (ΔSP). The cells were either treated with the proteasome inhibitor MG132 (10 μM for 6 h) or left untreated, and PrP levels were assessed by western blotting. Our results show that, whereas aggregated PrP accumulated in MG132-treated cells that expressed the wt SP-PrP or the ΔSP-PrP constructs (upper band), a much lower amount of aggregated PrP could be seen in MG132-treated cells that expressed the Prl SP-PrP or Opn SP-PrP molecules (Fig. S1D). The accumulation and aggregation of ΔSP-PrP in MG132-treated cells suggests that this construct is digested by the UPS and not by an alternative degradation pathway as shown for other PrP molecules (Hessa et al., 2011) [the bands that appear in all lanes (including ΔSP-PrP) above the area that is labeled 'Glycosylated PrP' are not specific]. The same experiment (Fig. S1D) also indicates that non-tagged PrP species that bear the wt PrP, Prl or Opn ER localization signals, undergo glycosylation. In contrast, ΔSP-PrP showed no glycosylation. These observations further confirm the efficiency of the Opn and Prl ER localization signals, and the inability of the ΔSP-PrP molecules to enter the ER.

Using the aforementioned fluorescently tagged PrP constructs, we tested whether the entry of PrP into the ER is a prerequisite for its deposition in a CsA-induced aggresome. To address this, we treated CHO cells that stably expressed the wt SP-YFP-PrP, Prl SP-YFP-PrP, Opn SP-YFP-PrP or ΔSP YFP-PrP molecules with 60 μg/ml CsA, the proteasome inhibitor MG132 (10 μM) or with both drugs, and visualized the cells by performing fluorescence microscopy. Although the inhibition of cyclophilin activity with CsA induced the formation of aggresomes in cells that expressed the wt SP-YFP-PrP, Prl SP-YFP-PrP or Opn SP-YFP-PrP constructs, no such phenomenon could be seen in CsA-treated ΔSP YFP-PrP-expressing cells (Fig. 1C).

To further examine whether the entry into the ER is required for the deposition of PrP in aggresomes and to test whether this phenomenon emanates from the addition of YFP to PrP, we transiently expressed the non-tagged PrP species in naïve CHO cells. The cells were treated with CsA, MG132 or both drugs as described above, and PrP was visualized by immunofluorescence. We found that non-tagged PrP molecules that had ER localization signals accumulated in aggresomes of CsA-treated cells but PrP molecules that lacked such signals did not do so (Fig. 1D; Fig. S1E).

These observations show that the formation of the PrP aggresome upon CsA treatment requires PrP entry into the ER, and indicate that the attachment of fluorescent tags to the protein does not affect sorting and deposition of PrP in the aggresome. These data also implicate cyclophilin B, an ER-resident cyclophilin, as the chaperone which is crucially needed for the correct folding of PrP.

To examine this notion, we used cyclophilin-B-knockout mice (CyPB KO mice) (Cabral et al., 2014). Brains from six 6-month-old CyPB KO and of six age-matched wild-type siblings (three males and three females for each genotype) were homogenized and subjected to high-speed centrifugation to separate soluble PrP species from PrP aggregates. The levels of PrP in the soluble and insoluble fractions were assessed by western blot analysis using the IPC1 anti-PrP antibody, and band intensities were measured and
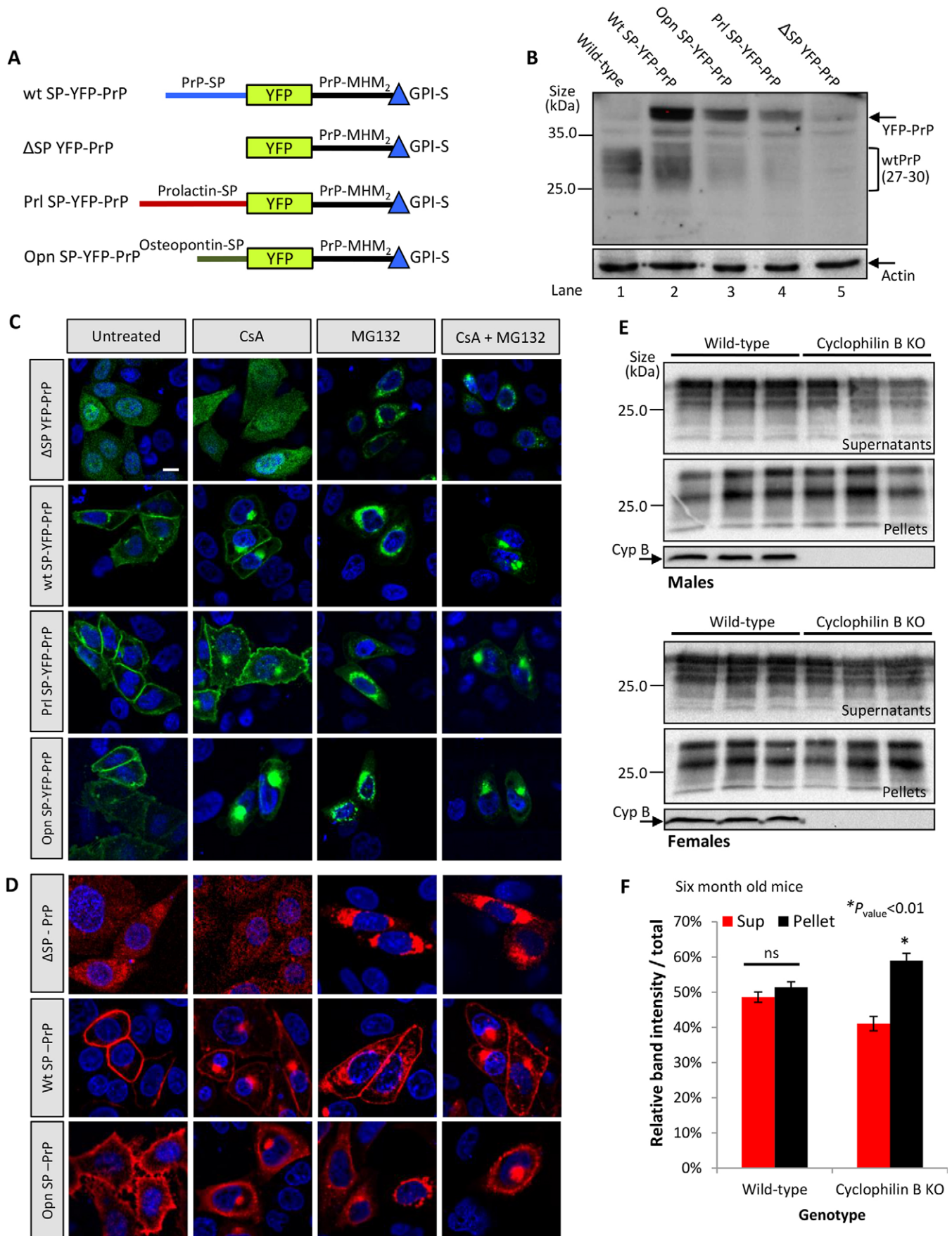
Fig. 1. See next page for legend.

Fig. 1. Entry to the ER is a prerequisite for the deposition of PrP in CsA-induced aggresomes. (A) Schematic illustrations of the different YFP-tagged PrP constructs used in this study. wt SP-YFP-PrP bears the natural PrP ER localization signal, ΔSP YFP-PrP lacks the ER localization signal and thus stays cytosolic, whereas Prl SP-YFP-PrP and Opn SP-YFP-PrP bear the ER localization signals of prolactin and osteopontin, respectively, and efficiently enter the ER. (B) Western blot analysis of all constructs described in A (3F4 PrP antibody was used). (C) CHO cells expressing one of the PrP constructs described in A (as indicated) were treated with MG132, CsA, both drugs, or left untreated. Unlike the cytosolic PrP isoform (ΔSP YFP-PrP), all PrP constructs that enter the ER accumulated in aggresomes of CsA-treated cells. In contrast, in MG132-treated cells the PrP constructs did not accumulate in aggresomes. Direct visualization of YFP fluorescence. Scale bar: 2 μm. (D) CHO cells expressing non-tagged PrP constructs that either bared the wt (wt SP-PrP) or Opn (Opn SP-PrP) ER localization signal or lacked such a signal (ΔSP-PrP) were treated with CsA, MG132 or both as in C. Immunofluorescence using a PrP antibody (3F4) unveiled that the non-tagged PrP species that had an ER localization signal were deposited in aggresomes as a result of CsA treatment but not after proteasome inhibition by MG132. Nuclei in C and D are stained with DAPI (blue). (E,F). Brains of six 6-month-old CyPB KO mice and six age-matched control animals were homogenized and subjected to high-speed sedimentation. PrP in supernatants and pellets was analyzed by western blotting using the IPC1 antibody (E). The absence of cyclophilin B resulted in increased PrP aggregation rates in the brains. Band intensity analysis (F) by the ImageJ software confirmed the significance of this phenomenon. *$P<0.01$; ns, not significant (two-tailed t-test).

compared. We found that animals that lacked cyclophilin B had more aggregated and less soluble PrP compared to their wild-type counterparts (Fig. 1E). Quantification of band intensities indicated that this change is significant (Fig. 1F, $P<0.01$). Similar analysis of brains of 1-month-old CyPB KO and wild-type mice showed no difference in the levels of soluble and aggregative PrP, implying that the aggregation of PrP is associated with age (Fig. S1F).

Cytosolic PrP species are not deposited in pre-existing aggresomes

Next, we examined whether cytosolic PrP molecules could be deposited in an existing aggresome despite their inability to induce *de novo* aggresome formation. YFP in the Opn SP-YFP-PrP construct was replaced with the red fluorescent protein mCherry (Shaner et al., 2004) to obtain red-labeled PrP molecules that efficiently entered the ER (Opn SP-RFP-PrP). Opn SP-RFP-PrP was transiently expressed in CHO cells that stably expressed ΔSP YFP-PrP, and the cells were treated with CsA for 5 h and visualized with a live-imaging technique. This setup enabled us to concurrently follow the cellular distribution of cytosolic PrP molecules (Fig. 2A, yellow) and of PrP molecules that efficiently entered the ER (red). As expected, red PrP molecules that passed through the ER accumulated in aggresomes of CsA-treated cells (Fig. 2A, arrows). However, cytosolic PrP species (yellow) did not accumulate in this pre-existing deposition site even 15 h after the exposure to CsA (see also Movie 1). Similar results were obtained when MG132 was added to the cell medium of a parallel experiment (Fig. S2A).

To further examine whether cytosolic PrP molecules can be deposited in existing aggresomes, we relied on the observation that aggresome-resident PrP molecules are constantly degraded (Ben-Gedalya et al., 2011). Thus, if cytosolic PrP molecules are not deposited in pre-existing aggresomes, it would be expected that the prevention of nascent PrP polypeptides from entering the ER, through blockage of the Sec61 translocon, would result in aggresome disintegration over time. First we examined whether Decatransin and HUN-7293, two efficient blockers of the Sec61 translocon (Junne et al., 2015), prevented PrP from entering the ER

in the presence and absence of CsA. Neuroblastoma 2a cells that stably expressed the PrP-MHM₂ construct (N2a-M cells) were treated for 16 h with CsA, Decatransin, HUN-7293, CsA+Decatransin, CsA+HUN-7293 or left untreated, and were then lyzed and subjected to high-speed centrifugation to sediment aggregated material. Supernatants were subjected to western blot analysis to detect PrP. Although mainly glycosylated PrP species were present in untreated cells, both glycosylated and non-glycosylated molecules were seen in CsA-treated cells (Fig. S2B, lanes 1 and 2, respectively). In contrast, most PrP species of Decatransin, HUN-7293, CsA+Decatransin and CsA+HUN-7293-treated cells were non-glycosylated (lanes 3–6). These observations demonstrate that Decatransin and HUN-7293 efficiently inhibit the entry of PrP into the ER of N2a-M cells.

Next, we tested whether blocking the translocon prevents the deposition of newly synthesized PrP molecules in pre-existing aggresomes. CHO cells expressing wt SP-YFP-PrP were treated with CsA for 16 h to induce the formation of aggresomes. CsA was washed out and either Decatransin or HUN-7293 was added to the cell medium. The translation inhibitor cycloheximide (Obrig et al., 1971) was added to another well, serving as a control for aggresome disintegration (Ben-Gedalya et al., 2011), and in another well the cell medium was supplemented solely with the vehicle (untreated). By employing live-imaging technique, we followed the fate of aggresomes for 8 h after adding the inhibitors. As expected, during this time window, the inhibition of translation by cycloheximide led to the disintegration of the aggresome whereas the washout of CsA had no detectable effect on these deposits (Fig. 2B). Similarly, blocking of Sec61 by either Decatransin or HUN-7293 also led to the disintegration of PrP aggresomes (Fig. 2B,C) confirming that PrP molecules that fail to enter the ER cannot be deposited in the aggresome. Importantly, this experiment also pointed out that cytosolic PrP molecules that bear the natural ER localization signal of the protein cannot reach the aggresome.

To further examine the role of the ER in the direction of misfolded PrP to the aggresome, we asked whether the inhibition of p97 (also known as VCP), an ATPase that is crucial for the retro-translocation of proteins from the ER to the cytosol (Xia et al., 2016), leads to aggresome disintegration. To address this, we induced the formation of aggresomes by treating CHO cells with CsA for 16 h followed by the exposure of the cells to the p97 inhibitors DBeQ or Eeyarestatin I. Live visualization unveiled that preventing PrP from exiting the ER also led to the disintegration of PrP-containing aggresomes (Fig. 2B, DBeQ, Fig. 2D; Fig. S2C, Eeyarestatin I).

Finally, we asked whether PrP molecules that carry the natural ER localization signal but fail to enter the ER, accumulate in aggresomes when proteasomes are inhibited. To test this, we first exposed CHO cells that express the MHM₂ PrP construct (CHO-M) for 16 h to the following treatments: CsA, MG132, Decatransin+MG132, Decatransin+MG132+CsA, HUN-7293+MG132 or HUN-7293+MG132+CsA. The cells were harvested and subjected to western blot analysis using the 3F4 antibody (Fig. S2D). Our results indicated that treating the cells solely with MG132 resulted in elevated levels of aggregated, glycosylated and unglycosylated PrP whereas combined treatments with Decatransin and MG132 or with Decatransin, MG132 and CsA mainly led to the accumulation of unglycosylated PrP. Similar results were observed when the Sec61 translocon was blocked with HUN-7293 (Fig. S2D). These results confirm that Decatransin and HUN-7293 inhibit the entry of PrP molecules into the ER of CHO-M cells, and have no observable effect on PrP translation.
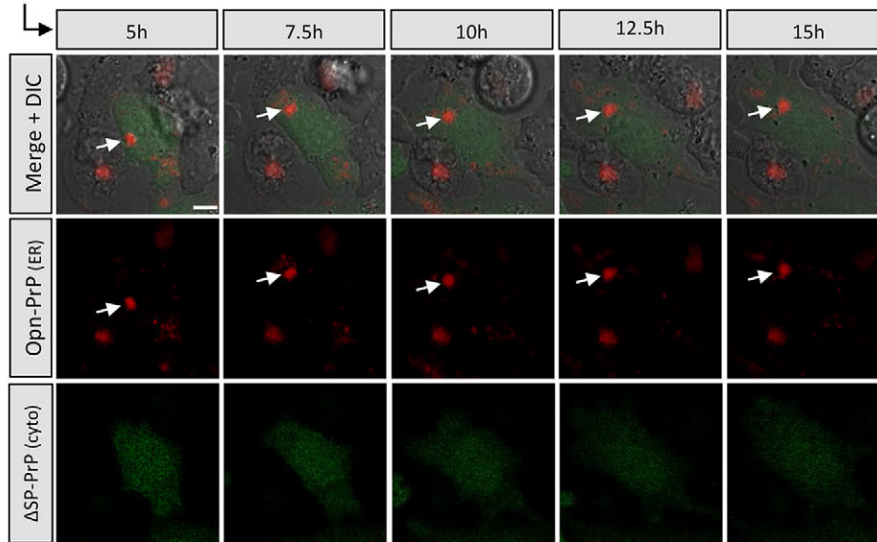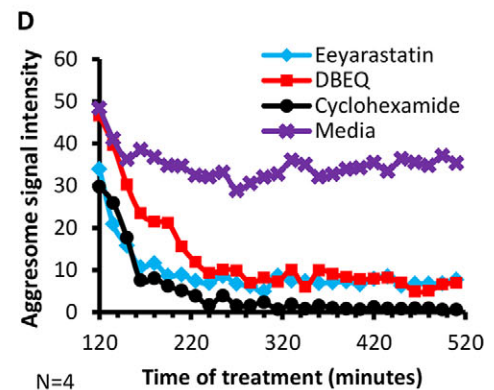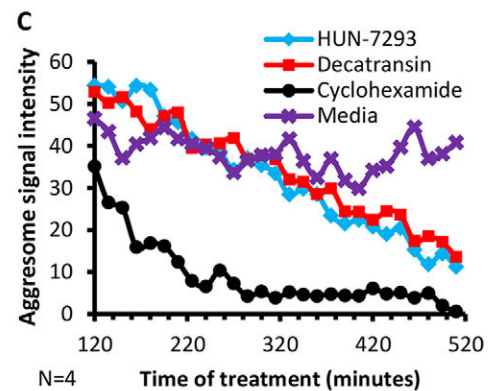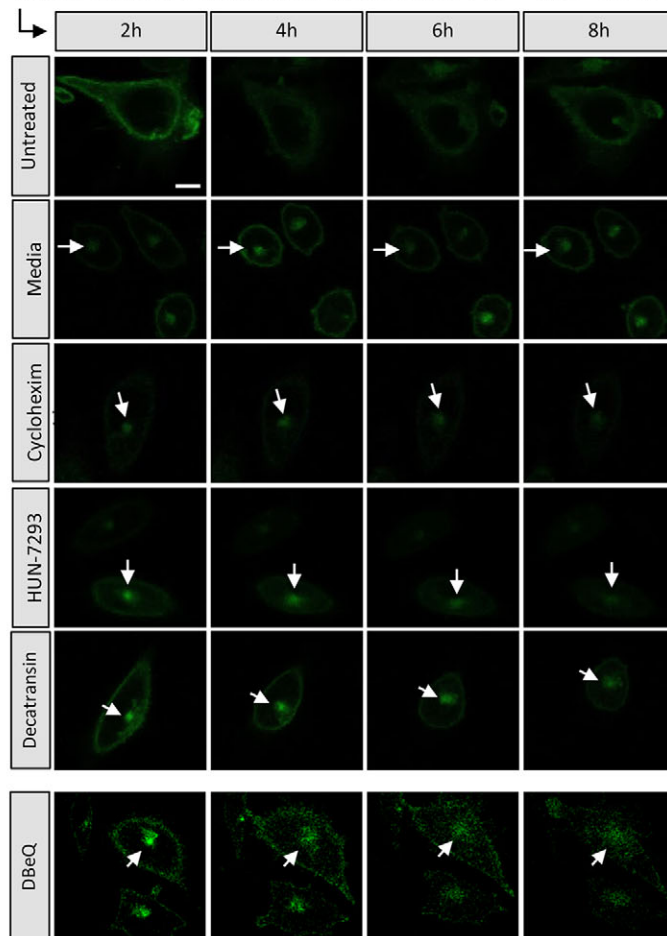
Fig. 2. Cytosolic PrP molecules do not accumulate in pre-existing aggresomes. (A) Live visualization of CsA-treated CHO cells expressing Opn SP-RFP-PrP (transiently) and the ΔSP-YFP-PrP (stably) shows that cytosolic PrP (yellow) molecules do not accumulate in pre-existing aggresomes (red, arrow). (B) CHO cells expressing wt SP-YFP-PrP were incubated for 16 h with CsA to induce aggresome formation. CsA was washed out and the Sec61 blockers Decatransin or HUN-7293, or the translation inhibitor cycloheximide (CHX), or the p97 inhibitor DBeQ were added to the cell medium. Aggresomes (arrows) were followed for 8 h after the addition of the compounds. Similarly to the inhibition of translation, blocking the Sec61 translocon and the inhibition of p97 led to aggresome disintegration. The concentrations of the added components were: decatransin (1 μm), HUN-7293 (1 μm), cyclohexemide (20 μg/μl), DBeQ (5 μm) and Eeyarastatin (5 μm). Scale bars: 2 μm. (C,D) Images of aggresome-containing cells were taken at 15-min intervals for 8.5 h. The mean fluorescent signal intensities of four aggresomes per treatment [as measured by the ImageJ software; CHX, Decatransin or HUN-7293 (C) or CHX, DBeQ or Eeyarastatin (D)] show constant decline in aggresome signal intensity as a result of Sec61 blocking (C) or p97 inhibition (D).

Next, we treated CHO cells expressing the wt SP-YFP-PrP construct with combinations of Sec61 inhibitors and CsA, or of either one of the inhibitors along with CsA and MG132, precisely as done in the experiment presented in Fig. S2D (see Fig. S2E for details), to further test whether the prevention of PrP entry into the ER reduces the amount of aggresomes within the cell populations. Aggresomes were counted in at least 100 cells per treatment. Our results (Fig. S2E) show that the inhibition of Sec61 led to a remarkable decrease in the number of aggresomes in all cell populations.

Taken together, our results show that the entry and exit of PrP molecules into and out of the ER are prerequisites for their accumulation in the aggresome of CsA-treated cells.

The Golgi has no role in the direction of PrP to CsA-induced aggresomes

After being processed in the ER, newly synthesized PrP molecules are transported to the Golgi for additional maturation steps. Thus, we examined whether the Golgi has any role in the direction of PrP to the aggresome or whether the decision to direct CsA-induced misfolded PrP species is solely taken within the ER. To test this, we used the fungal metabolite Brefeldin A (BFA), which inhibits vesicular transport from the ER to the Golgi, an inhibition that results in the collapse of the Golgi cisterns into the ER (Misumi et al., 1986). First, we calibrated the BFA concentration and time of exposure required for a complete collapse of the Golgi into the ER by co-transfecting two plasmids into CHO cells; one that carries a GalT gene fused to YFP (GalT–YFP), serving as a Golgi marker (Yang and Storrie, 1998) and a plasmid that carries a gene encoding for the red fluorescent protein DsRed fused to the ER retention signal KDEL (Munro and Pelham, 1987), thereby labeling the ER. We found that treating cells with 1 nM BFA for 6.5 h was sufficient to confer a complete collapse of the Golgi into the ER (Fig. S3A).

Using CHO cells expressing the wt SP-YFP-PrP, we examined whether CsA induces the formation of aggresomes in the absence of Golgi. The cells were either left untreated or incubated for 6.5 h with 60 µg/ml CsA, 1 nM BFA, or with both drugs (CsA+BFA). After treatment, the cells were fixed, labeled with an anti-vimentin antibody (Fig. 3A, red) and visualized. PrP-containing aggresomes were observed in cells treated solely with CsA, but the treatment with BFA alone led to the accumulation of wt SP-YFP-PrP in the ER and cytosol but not in aggresomes (Fig. 3A, BFA). However, well-defined PrP-containing foci were seen in cells that were treated with both drugs (CsA+BFA). The observations that vimentin confined these foci (CsA+BFA, inset) and that these structures colocalized with the MTOC [labeled by a γ-tubulin antibody (Fig. 3B, arrows)] confirmed that PrP accumulated in aggresomes despite the absence of the Golgi complex. This indicates that the Golgi has no role in directing CsA-induced misfolded PrP molecules to the aggresome. Given that BFA induces ER stress and activates the ER unfolded protein response, we exposed identical wt SP-YFP-PrP-expressing CHO cells to an additional inducer of ER stress, dithiothreitol (DTT) (Oslowski and Urano, 2011) and observed no aggresomes (Fig. S3B). This implies that the activation of ER unfolded protein response is not sufficient to induce the formation of PrP aggresomes.

A GPI moiety is required for the direction of PrP to CsA-induced aggresomes

Given that aggresome-resident PrP species originate exclusively from the ER, we asked which processing steps within this organelle are prerequisites for the deposition of a PrP molecule in this
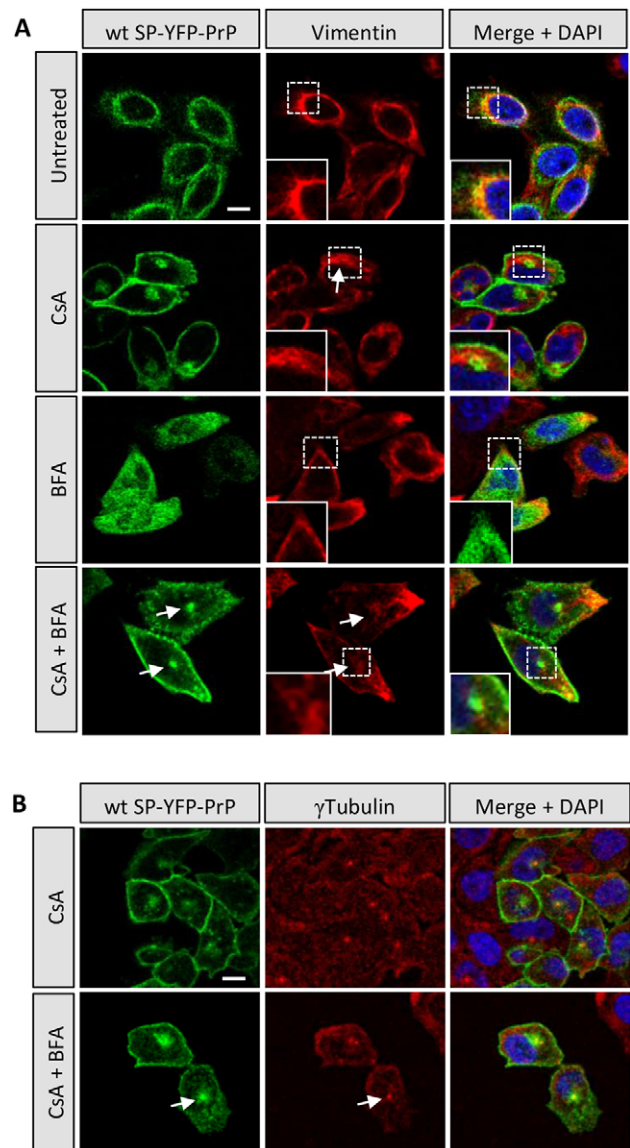

Fig. 3. The Golgi complex plays no role in the direction of PrP to aggresomes. (A) CHO cells expressing the wt SP-YFP-PrP construct were treated with CsA, Brefeldin A (BFA), with both compounds or left untreated. Vimentin was labeled with a specific antibody (red). Unlike CsA, BFA did not induce the formation of PrP-containing aggresomes. However, aggresome formation was not prevented when cells were treated with both drugs (CsA+BFA, arrows). (B) Aggresomes of cells that were treated with both CsA and BFA colocalized with the MTOC (arrow, labeled with a γ tubulin antibody, red). Insets show a magnified image of the indicated region. Nuclei are stained with DAPI (blue). Scale bars: 3 µm.

structure. First, we tested whether CsA-induced misfolded PrP molecules bear a GPI tail. We subjected N2a-M cells to preparative floatation and collected the upper fractions, which contain detergent-resistant membrane micro-domains (DRMs) and fully processed PrP molecules (Naslavsky et al., 1997) (Fig. S4A). These mature PrP molecules have passed through the ER and the Golgi and thus, lack the ER localization signal, bear the GPI tail and are glycosylated (Fig. 4A, lane 1). To use these molecules as size markers for non-glycosylated PrP, we removed their glycans using PNGase F (lane 2, band 'A'). High-speed pellets of N2a-M cells that were treated with CsA (lane 3) or left untreated (lane 4), as well as of untreated N2a cells that expressed the ΔSP-PrP-MHM$_2$ construct
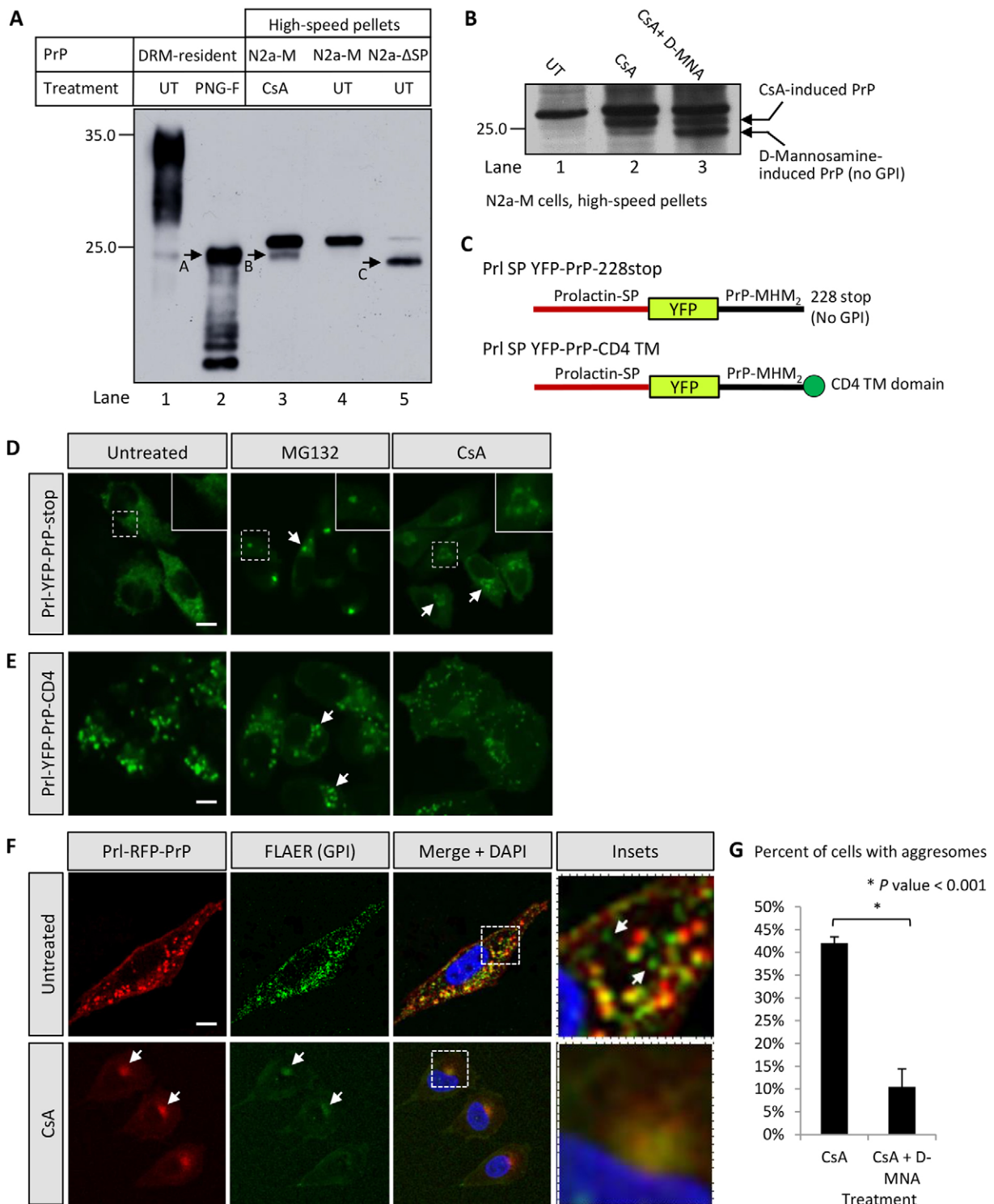
Fig. 4. See next page for legend.

(lane 5), were also prepared. Western blot analysis revealed that CsA treatment induced the appearance of a new aggregative PrP band (lane 3, 'B') that migrated identically to the mature unglycosylated PrP (lane 2, 'A'). PrP molecules that lacked the ER localization signal (and thus, also lack the GPI anchor) were smaller in size compared to the CsA-induced PrP (lane 5 band 'C'). These results suggest that CsA-induced aggregative PrP molecules that lack the ER localization signal but bear the GPI anchor enter the ER. They

also raise the possibility that aggresome-resident PrP molecules bear the GPI moiety.

To test this assumption, we used D-mannosamine (D-MNA), a compound that inhibits the attachment of GPI to proteins (Lisanti et al., 1991). N2a-M cells were either left untreated, treated with CsA or with both CsA and D-MNA and subjected to high-speed centrifugation. The PrP content in pellets of all three samples were analyzed by immunoblotting (Fig. 4B). Whereas CsA-induced PrP

Fig. 4. CsA leads to the accumulation of GPI anchored PrP species in the aggresome. (A) Neuroblastoma 2a cells expressing the MHM$_2$ PrP construct (N2a-M cells) were subjected to preparative floatation to isolate mature PrP molecules, which were left untreated (lane 1) or treated with PNGase F (lane 2). Mature, unglycosylated PrP, lacking the ER signal peptide but bearing a GPI moiety are labeled as band 'A'. Similar N2a-M cell populations were left untreated (UT) or incubated with CsA, homogenized and subjected to high-speed centrifugation. Pellets of CsA-treated (lane 3) and of untreated cells (lane 4) were separated on the gel. CsA treatment resulted in the formation of insoluble PrP conformers (band 'B') that migrated identically to the mature, unglycosylated, GPI-bearing PrP (band 'A'). N2a cells expressing PrP that lacked the ER localization signal (N2a-ΔSP cells) were subjected to high-speed centrifugation to obtain insoluble PrP molecules that lacked both the ER localization peptide and the GPI moiety. These molecules (lane 4, band 'C') were smaller in size than the CsA-induced PrP species (band 'B'). (B) N2a-M cells were left untreated, incubated with CsA or treated with both CsA and D-mannoseamine (D-MNA). The cells were homogenized, subjected to high-speed centrifugation and PrP conformers were blotted using a PrP antibody (clone 3F4). CsA induced the formation of an insoluble PrP conformer (lane 2) that was smaller than PrP in untreated cells (lane 1), but larger than the lower band seen in cells treated with both drugs (lane 3). (C) Schematic illustrations of Prl SP-YFP-PrP-228stop and of Prl SP-YFP-PrP-CD4 TM. (D) CHO cells expressing Prl SP YFP-PrP-228stop were treated with either MG132 or CsA. Neither one of these drugs induced the formation of PrP aggresomes. Arrows point at non-aggresomal PrP deposits. (E) Prl-YFP-PrP-CD4 accumulated in numerous foci in CHO cells (arrows) regardless of whether the cells were treated with CsA, MG132 or left untreated. (F) Prl SP-RFP-PrP-expressing CHO cells were left untreated or incubated with CsA and GPI was labeled with FLAER. FLAER signals were observed in both CsA-induced aggresomes (arrows) and on the cell surface (insets). Insets show a magnified image of the indicated region. Scale bars: 3 µm. (G) wt SP-YFP-PrP-expressing CHO cells were treated with CsA or with both CsA and D-MNA and the numbers of aggresomes were counted in the cell populations (more than 100 cells from three or four different microscopic fields per treatment). Whereas ∼43% of the CsA-treated cells contained PrP aggresomes only ∼10% of the cells that were treated with both drugs contained aggresomes. *$P<0.001$ (Student's t-test (paired, two-tail analysis).

species (lane 2) appeared to be slightly smaller than those seen in untreated cells (lane 1), concurrent treatment with CsA and D-MNA induced the appearance of an additional PrP band that was smaller than the CsA-induced PrP (lane 3) suggesting that CsA-induced aggregative PrP molecules bear the GPI anchor.

Next, we tested whether preventing the attachment of GPI to PrP impaired the deposition of the molecules in aggresomes of CsA-treated cells. To address this, we inserted a stop codon at residue 228 of Prl SP-YFP-PrP to obtain PrP molecules that enter the ER but are incapable of acquiring the GPI tail (Prl-YFP-PrP-228stop) (Fig. 4C). The inhibition of glycosylation has been reported to not impair the attachment of GPI anchor to PrP (Winklhofer et al., 2003) indicating that the attachment of GPI occurs prior to glycosylation. Thus, we expected that PrP molecules that lack the GPI anchor would enter the ER but stay unglycosylated. To test this, we stably expressed the wt SP-PrP-228stop PrP construct in CHO cells, subjected them to western blot analysis and found that these molecules were not glycosylated regardless of whether proteasomes were inhibited or not (Fig. S1D). To assess whether wt SP-PrP-228stop PrP molecules accumulated in aggresomes upon CsA treatment, we treated the cells with CsA or MG132 and visualized them by fluorescent microscopy. In untreated cells, Prl-YFP-PrP-228stop molecules were distributed throughout the cell (Fig. 4D, untreated) but seemed not to reach the cell surface (inset). This observation suggests that these molecules were trapped within the ER. Proteasome inhibition mediated by MG132 resulted in the accumulation of these molecules in foci. Nonetheless, these structures differed from aggresomes, as they were not adjacent to the nucleus and more than one PrP deposit was present in most cells (Fig. 4D, MG132, arrow and inset). Interestingly, CsA treatment

resulted in the accumulation of Prl-YFP-PrP-228stop in a juxta-nuclear ring-like structure with morphology different from that of aggresomes (Fig. 4D, CsA, arrows and inset). A more detailed characterization of these structures is needed to elucidate their features. The redistribution of Prl-YFP-PrP-228stop in CsA-treated cells and the lack of effect of CsA on the distribution of ΔSP-PrP (Fig. 1C) imply that Prl-YFP-PrP-228stop molecules enter the ER. However, the observation that neither proteasome inhibition nor CsA treatment directed Prl-YFP-PrP-228stop molecules to aggresomes indicates that the anchorage of PrP to the ER membrane is required for the direction of PrP to aggresomes. These results led us to ask whether another anchoring sequence is capable of restoring the deposition of Prl-YFP-PrP in aggresomes or whether the GPI anchor has a unique role in this process.

To test whether the attachment of PrP to the membrane is sufficient for the transportation of PrP to aggresomes, we replaced the GPI attachment signal of Prl SP-YFP-PrP with the transmembrane domain of the cluster differentiation 4 (CD4) (Prl-YFP-PrP-CD4, Fig. 4C; for the sequence, see Fig. S4B). The cells were either left untreated, or treated with MG132 or CsA as described above, and visualized by fluorescence microscopy. Prl-YFP-PrP-CD4 molecules accumulated in punctate patterns in all cell populations (Fig. 4E). The glycosylation of wt SP-PrP-CD4 molecules (Fig. S1D) strongly suggests that they accumulate within the ER. These results indicate that the attachment of PrP to the ER membrane by the mouse CD4 transmembrane domain is not sufficient to promote their direction to the aggresome upon CsA treatment.

We next examined whether aggresome-resident proteins bear a GPI anchor or whether this moiety is cleaved prior to their deposition in this site. To address this, we used Alexa-Fluor-labeled aerolysin (FLAER), a reagent that specifically labels GPI-bearing proteins (Brodsky et al., 2000). CHO cells expressing Prl SP-RFP-PrP were treated with CsA, fixed, labeled with FLAER and visualized through confocal microscopy. We found that PrP-containing aggresomes encompassed GPI-anchored proteins (Fig. 4F, green). In contrast, PrP aggresomes of non-permeabilized cells were not labeled with FLAER (Fig. S4C), confirming that this reagent reacted with cytosolic foci.

To further scrutinize whether the GPI anchor of PrP is required for its deposition in the aggresome, we asked whether the inhibition of GPI attachment reduces the number of aggresome-containing cells in the population. Visualization of CHO cells expressing wt SP-YFP-PrP that were treated with both CsA and D-MNA unveiled that whereas ∼43% of the cells that were treated solely with CsA contained PrP aggresomes, only 10% of the cells that were exposed to CsA and D-MNA contained these structures (Fig. 4G).

Collectively our observations indicate that the attachment of a GPI anchor is required for the deposition of PrP in CsA-induced aggresomes, and reinforce the conclusion that an ER-resident mechanism directs misfolded PrP to the cytosolic aggresome upon the inhibition of cyclophilin B.

Differential effects of N-linked glycosylation on the deposition of PrP in aggresomes

Two asparagine residues in the sequence of PrP, at N180 and N196, serve as N-linked glycosylation sites. A previous study has shown that at least 50 different sugar chains can be attached to these sites (Endo et al., 1989), which are probably important for prion toxicity (reviewed in Lawson et al., 2005). Indeed, the inhibition of complex glycosylation accelerates the formation of toxic PrP conformers in cultured cells (Winklhofer et al., 2003), and

PrP molecules that cannot undergo glycosylation are targeted for ERAD-mediated degradation (Shao et al., 2014). Therefore, does glycosylation play a role in the deposition of PrP in aggresomes of CsA-treated cells?

To address this question we replaced the asparagine residues of wt SP-YFP-PrP to obtain fluorescently tagged PrP molecules that cannot undergo glycosylation on either residue 180 (wt SP-YFP-N180Q-PrP) or 196 (wt SP-YFP-N196Q-PrP) (Fig. 5A). Western blot analysis of cells that stably expressed the glycosylation mutants revealed that both mutated PrP molecules underwent partial glycosylation that can be removed by PNGase F (Fig. 5B).

To test whether glycosylation is required for the direction of PrP to aggresomes, CHO cells expressing these mutated PrP species were left untreated or incubated with CsA and visualized as described above. Unexpectedly, we observed distinct distribution patterns for the two different glycosylation mutants. wt SP-YFP-N180Q-PrP molecules accumulated in large juxta-nuclear structures (possibly the Golgi) and did not reach the cells surface regardless of whether the cells were treated with CsA or left untreated (Fig. 5C, arrowheads). In contrast, wt SP-YFP-N196Q-PrP molecules arrived

at the surface of untreated cells and accumulated in aggresomes upon CsA treatment (Fig. 5C, arrows).

These results show that the inability to glycosylate PrP on residue 180 impedes proper maturation of the protein. Nevertheless, it is possible that PrP molecules that fail to be glycosylated on residue 180 can reach the Golgi even if cyclophilins are inhibited by CsA. Intriguingly, the replacement of N196 with Q (N196Q) had no effect on the distribution of the protein in untreated and in CsA-treated cells. This finding corroborates a previous study that reported that the mutation of N196 does not impair the cellular trafficking of PrP (Winklhofer et al., 2003).

DISCUSSION
In this study, we utilized the phenomenon of PrP accumulation in aggresomes of CsA-treated cells despite intact proteasome activity to investigate the cellular pathway through which PrP is directed to these structures. Whereas most nascent PrP molecules are co-translationally translocated into the ER through the Sec61 complex (Fig. 6, I), a small sub-population stays cytosolic and is rapidly digested by proteasomes (Drisaldi et al., 2003) (Fig. 6, II). Our results
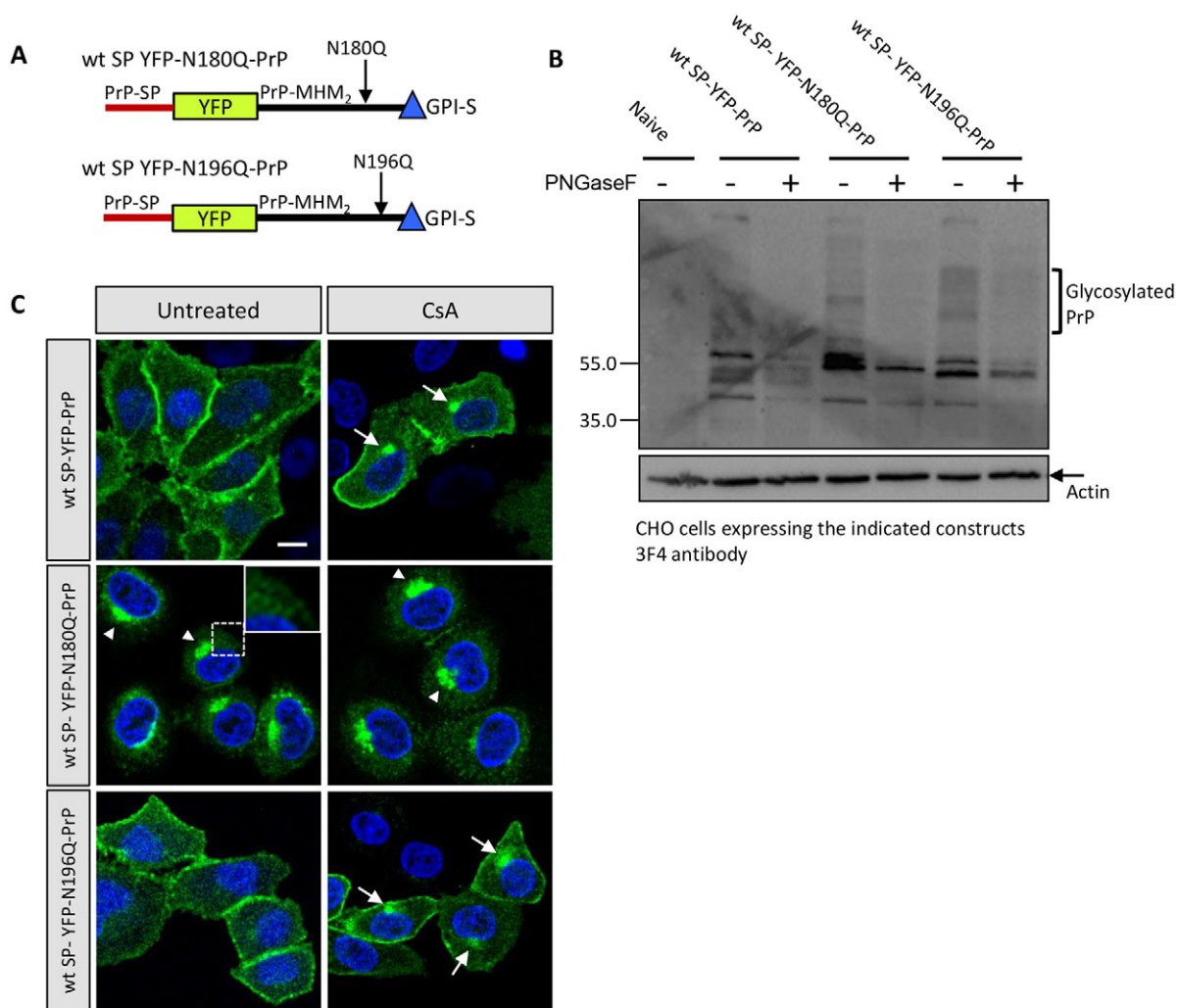

Fig. 5. Differential effects of N-linked glycosylation on PrP deposition. (A) Illustrations of PrP glycosylation mutants: wt SP YFP-N180Q-PrP and wt SP YFP-N196Q-PrP. (B) CHO cells stably expressing the glycosylation PrP mutants were harvested and treated with PNGase F or not. Western blotting analysis shows that both mutants undergo partial glycosylation. (C) The mutation N180Q prevents PrP from reaching the cell membrane (inset) leading to its accumulation in non-aggresomal structures (possibly the Golgi) in both untreated and CsA-treated CHO cells (arrowheads). In contrast, the N196Q mutation does not alter the cellular trafficking of PrP. It reaches the surface of untreated cells and accumulates in aggresomes of CsA-treated cells (arrows). Insets show a magnified image of the indicated region. Direct visualization of YFP fluorescence; nuclei were stained with DAPI (blue). Scale bar: 3 µm.
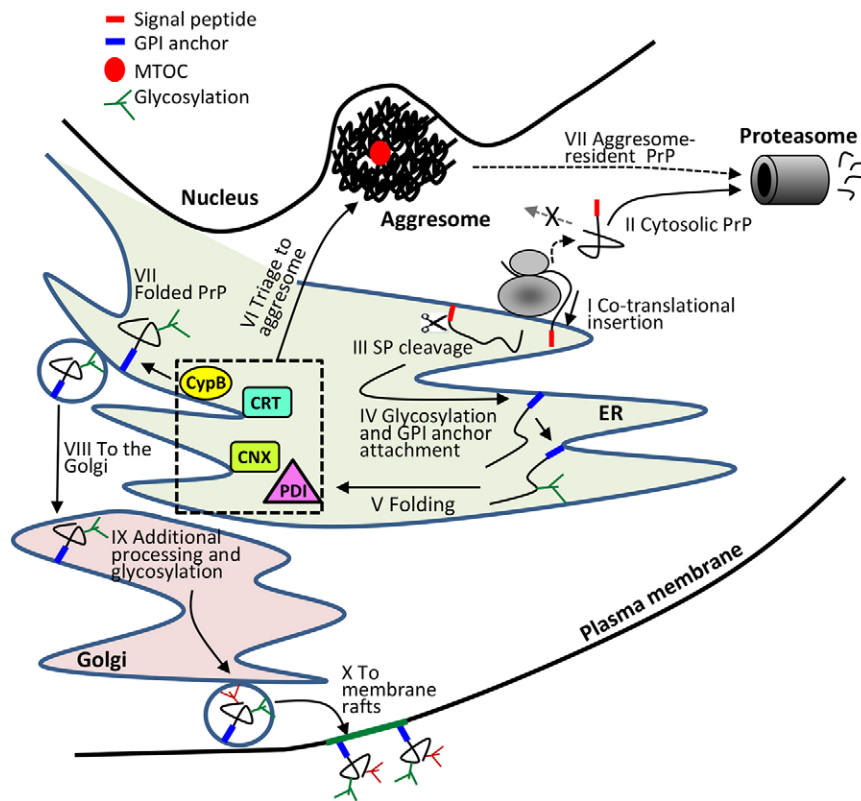
Fig. 6. A model of PrP processing and maturation in the cell. Similar to other secreted proteins, the majority of nascent PrP molecules co-translationally enter the ER (I). However, a small subpopulation that stays cytosolic is digested by proteasomes (II). In the ER, the ER localization signal is cleaved (III), a GPI anchor is attached to the C-terminus of PrP and the protein is glycosylated (IV). Next, the protein undergoes a series of folding events (V) that are catalyzed by the folding chaperones including calnexin (CNX), calreticulin (CRT), protein disulfide isomerase (PDI) and cyclophilin B. Molecules that fail to be assisted by cyclophilin B are retro-translocated to the cytosol and deposited in the aggresome (VI). PrP molecules that complete the folding process successfully (VII) are transported to the Golgi (VIII) where they undergo glycosylation and additional maturation steps (IX). Mature molecules are exported to be presented on membrane rafts of the cell surface (X).

show that the entry into the ER is a prerequisite for the deposition of PrP in the aggresome and that cytosolic molecules are not deposited even in a pre-existing aggresome (Fig. 2). Shortly after the translocation of the nascent PrP polypeptide into the ER, its ER localization signal peptide is cleaved (Fig. 6, III), a GPI anchor is attached to the protein and early glycosylation occurs (Fig. 6, IV). Interestingly, the addition of a GPI anchor is crucial for the deposition of PrP to the aggresome (Fig. 4) but glycosylation has no crucial role this process (Fig. 5). Next, the premature PrP molecule undergoes a series of chaperone-assisted folding events within the ER (Fig. 6, V). Our mouse-based experiments suggest that a failure of cyclophilin B to catalyze the isomerization of PrP from cis to trans leads to the shuttling of the molecule to the aggresome (Fig. 6, VI). We also found that, despite its well-documented roles in the proper maturation of PrP, the Golgi is not required for the direction of CsA-induced misfolded PrP molecules to the aggresome (Fig. 3) indicating that the triage of PrP to the aggresome occurs within the ER. This observation is surprising as it has been previously shown that certain disease-linked PrP mutants are directed for degradation through the Golgi (Ashok and Hegde, 2009), implying that distinct quality control mechanisms supervise the folding of different PrP mutants.

The appearance of 25-kDa PrP molecules in CsA-treated cells, the indistinguishable migration of these molecules and of mature GPI-bearing unglycosylated PrP (Fig. 4A), and the presence of GPI in the aggresome (Fig. 4F) suggest that the 25-kDa PrP species are the molecules that accumulate in the aggresome. Nevertheless, we have no direct evidence that this is the case and further research is needed to clarify this issue.

The inhibition of ER-resident cyclophilins directs PrP to the aggresome
Our discoveries show that the triage of misfolded PrP molecules to the aggresome occurs within the ER and specifically point at

cyclophilin B as a key player in this quality control and sorting mechanism. In this context, it is plausible that the attachment of a GPI moiety to the newly synthesized PrP molecule is required for its processing by specific folding chaperones and consequently for its deposition in the aggresome when it fails to fold properly. However, it is apparent that not all PrP-interacting folding chaperones are involved in this process. Whereas the failure of an ER-resident cyclophilin (Stocki et al., 2014) to interact with PrP leads to its deposition in the aggresome, inhibiting the activity of ERp57 (also known as PDIA3), a protein disulphide isomerase (PDI), has no effect on the deposition of PrP in the aggresome (Torres et al., 2015). The irrelevance of PDI in the triage of PrP to the aggresomes is also supported by the observation that preventing the formation of a disulfide bridge results in the accumulation of PrP in large non-aggresomal foci (Yanai et al., 1999). It is important to note that the deposition of different conformers of the same protein in distinct cellular sites is not unique to PrP. For instance, different Alzheimer's-disease-causing mutations in the protease presenilin-1 (PS1, also known as PSEN1) impede the protein from folding properly, but direct the misfolded conformers to distinct cellular compartments. Although PS1 that carries the A264E mutation accumulates in aggresomes (Johnston et al., 1998), the mutation of P264 or P267 leads to the deposition of PS1 in an ER-derived quality control compartment (ERQC) (Ben-Gedalya et al., 2015). It is unknown why specific misfolded protein conformers are deposited in an aggresome, whereas other mutants of the same protein accumulate elsewhere. One possibility is that the ER cannot retro-translocate certain highly disordered conformers to the cytosol and this confers their accumulation in the ERQC. It is also possible that relatively stable, hard to digest molecules are deposited in the aggresome where they undergo slow degradation, whereas conformers that can be easily digested are cleared by proteasomes upon exiting the ER.

Another intriguing discovery is the deposition of PrP 228stop in non-aggresomal foci (Fig. 5). This finding is consistent with the report that PrP forms aggregates in the brain of individuals who carry stop codons in residues Y226 or Q227 of *PRNP* and therefore express anchorless PrP (Jansen et al., 2010). The development of atypical GSS by the individual that carried the Q227stop mutation suggests that the formation of aggresomes is not necessarily associated with this disease, and strongly suggests that more than one mechanism can underlie the development of GSS.

Differential roles for N-linked glycosylation in protein quality control

An additional question is why different N-linked glycosylation mutants exhibit distinct features. N-glycans are attached to nascent proteins shortly after their translocation into the ER (Helenius and Aebi, 2004). This event is crucial for further modification by lectin-based chaperone systems (Noack et al., 2014). Thus, it was expected that the prevention of glycosylation following the mutation of asparagine residues would lead to the misfolding of PrP, its accumulation within the ER or its deposition in the aggresome. Nevertheless, we found that the mutation of asparagine 180 resulted in the accumulation of the protein in undefined foci in untreated and CsA-treated cells. These surprising results suggest that some types of misprocessed PrP molecules are able to leave the ER and raise the question of whether these molecules interact with cyclophilin B or not.

In contrast, PrP molecules that cannot be glycosylated on N196 exhibited no trafficking abnormalities, suggesting that this residue is dispensable for the correct folding of PrP or at least, does not induce the formation of a PrP form that is recognized by the ER mechanisms as misfolded. The presence of these molecules on the surface of untreated cells and their deposition in aggresomes upon CsA treatment strongly suggest that the absence of N196 does not hinder the interaction of PrP and cyclophilin B.

Potential clinical applications

Our study indicates that the correct folding of PrP requires functional interactions with cyclophilin B and that aggresomes serve as a component of an ER-resident quality control mechanism. The apparent link between GSS and failed interaction between PrP and cyclophilin B, as well as the possibility that aggresomes become sources of toxicity in late stages of life (Ben-Gedalya and Cohen, 2012), suggest that the stabilization of nascent PrP molecules in trans position by chemical chaperones could reduce the amounts of disease-causing PrP conformers, postpone the emergence of GSS in individuals who carry the P102L, or P105L or P105S mutations and slow its progression once emerged.

MATERIALS AND METHODS
Materials
Cell culture reagents were purchased from Biological Industries (Beit Haemek, Israel). G-418 was from Calbiochem (San Diego, CA). Protein concentration was determined by using a BCA kit (Pierce cat. no. 23223). Cloning was performed by using a QuikChange Lightning kit (Agilent cat. no. 210515). Alexa-Fluor-488-labeled proaerolysin (FLAER, cat. no. FL1S-C) was from Cedarlane (Burlington, ON, Canada). Cyclosporin-A (CsA) (cat. no. C1832), MG132 (cat. no. C2211), Brefeldin A (BFA) (cat. no. B7651), D-Mannosamine hydrochloride (D-MNA) (cat. no. M4670), Histodenz (cat. no. D2158), Dithiothreitol (DTT) (cat. no. D0632), DBeQ (cat. no. SML0031), Eeyarestatin I (cat. no. E1286), cycloheximide (CHX) (cat. no. C7698) and PNGase F (cat. no. G5166) were purchased from Sigma. Decatransin and HUN-7293 were supplied by Novartis (Basel, Switzerland).

Cell cultures and transfections
N2a and CHO cells stably expressing moderate levels of the different PrP constructs based on the MHM$_2$-PrP chimeric protein (Scott et al., 1992) were used. Cells were grown at 37°C in Dulbecco's modified Eagle's medium (DMEM) supplemented with 10% fetal calf serum. Stable transfections were achieved with the TransIT-LT1 (cat. no. MIR 2300) transfection reagent (Mirus, Madison WI) according to the manufacturer's instructions. Selections were performed using G-418 (0.35 mg/ml for N2a and 0.78 mg/ml for CHO cells). The cultures were regularly tested for mycoplasma contamination.

Plasmids
GalT–YFP was used to label the Golgi. pDsRed2-ER vector (Clontech, Mountain View CA, cat. no. 632409) was used to label the ER. The wt SP-YFP-PrP chimera is as described previously (Ben-Gedalya et al., 2011). The other constructs were created on the basis of the wt SP-YFP–PrP plasmid using the QuikChange Mutagenesis Kit (Agilent, Santa Clara, CA).

Antibodies
MHM2-PrP was detected using the 3F4 monoclonal antibody (mAb) (SIG-39600 Covance, Princeton NJ, USA) which was used for western blotting (1:5000) or for immunofluorescence (1:500). PrP in mouse brains was detected with the IPC1 antibody (Sigma cat. no. P5999, 1:1000). β-Actin mAb (A5441), γ-tubulin mAb (T6557) and vimentin mAb (V6630) were from Sigma and used for western blotting (1:20000) or immunofluorescence (1:200). Cyclophilin B antibody (Abcam cat. no. ab74173) was used for western blotting (1:2000). Secondary antibodies conjugated to Cy5 (cat. no. 715-175-150) or horseradish peroxidase (HRP) (cat. no. 715-035-151) were from Jackson ImmunoResearch (West Grove, PA).

Immunofluorescent microscopy and live imaging
To detect fluorescent PrP, cells were grown on poly-D-lysine-coated chamber slides (Nunc cat. no. 155411), fixed (10% formalin in PBS for 30 min at room temperature), mounted in an anti-fading preparation (5% *n*-propyl gallate, 100 mM Tris-HCl pH 9, 70% glycerol) or in Vectashield (cat. no. H1200; Vector Laboratories, Burlingame, CA) and viewed with a Zeiss LSM 710 Axio Observer confocal microscope using a 63×1.40 NA oil DIC lens. Images acquisition (except for live imaging) was performed at room temperature using the ZEN lite 2012 software. For immunofluorescence, cells were fixed, quenched with cold 1% NH$_4$Cl in PBS, permeabilized (0.1% Triton X-100 in PBS for 2 min at room temperature) and blocked with 2% BSA (30 min at room temperature). The cells were then incubated with the PrP primary antibody (in 1% BSA overnight at 4°C), rinsed, and the secondary antibody conjugated to Cy5 (diluted 1:300 in 1% BSA) was added for 30 min at room temperature. For visualizing FLAER, cells were either permeabilized (0.1% Triton X-100 in PBS for 2 min at room temperature) upon fixation or left unpermeabilized and incubated with 100 nM FLAER for 1 h (4°C). Labeled cells were mounted and visualized as described above.

For live imaging, cells were grown on either an eight-well μ-Slide, ibiTreat (ibidi GmbH cat. no. 122598, Munich, Germany) or 35-mm glass-bottom dishes (MatTek cat. no. P35GC-1.0-14-C, Ashland, MA). Clip acquisition was performed using the same microscopy system at 37°C.

PrP analysis
SDS-PAGE and western blotting of PrP were carried out as described previously (Taraboulos et al., 1995). Cells were lysed in ice-cold Triton-doc lysis buffer (0.5% Triton X-100, 0.25% Na-deoxycholate, 150 mM NaCl, 10 mM Tris-Cl, pH 7.5, 10 mM EDTA). The lysates were spun for 3 min at 2348 *g* in a desktop microfuge. Biochemical analyses were performed on the post-nuclear supernatant (PNS). Aggregated PrP was separated from the soluble fractions by a sedimentation procedure. The PNS was brought to 1% Sarkosyl, incubated on ice for 30 min and then spun for 1 h at 45,000 rpm at 4°C in a TL45 rotor (109,000 *g*). The pellets were resuspended in lysis buffer. Western blots were developed using an ECL system.

The analysis of PrP in the brain of CyPB KO mice

CyPB KO mice (Cabral et al., 2014) and their wild-type siblings (strain C57BL/6, which were bred from Het X Het mating) were maintained under an NICHD-approved animal care program. Mice were euthanized at either 1 or 6 months of age, and brains were removed. One hemisphere was homogenized and used for high-speed sedimentation assays. Brain homogenates were spun in a TLA45 rotor for 1 h at 45,000 rpm (109,000 g) at 4°C, supernatants were separated from pellets and PrP was analyzed by immunoblotting using the IPC1 antibody.

The blots were analyzed with the ImageJ software; the intensity of each lane was measured. Background intensity was subtracted from the measurements. Afterwards, the total intensity measurements of the supernatant and pellet for each mouse were added together. To obtain the relative amount of PrP molecules for each mouse separately, the measurement of either the supernatant or the pellet fractions were divided by the total amount in both fractions and plotted.

Flotation assay and deglycosylation of PrP

PNGase F experiments were performed on either purified DRMs or on the whole supernatant. For DRM isolation, confluent cells growing in two 10-cm plates were rinsed and scraped into cold PBS buffer prior to their lysis with 400 µl of lysis buffer (150 mM NaCl, 25 mM Tris-HCl pH 7.5, 5 mM ETDA, 1% Triton X-100). Lysates were adjusted to 35% Histodenz by adding an equal volume of ice-cold 70% Histodenz prepared in TNE (25 mM Tris, pH 7.5, 150 mM NaCl, 5 mM EDTA) and loaded at the bottom of Beckman Instruments TLS-55 ultracentrifuge tubes. A 8–35% Histodenz linear step gradient in TNE was then overlaid above the lysate (200 µl each of 25, 22.5, 20, 18, 15, 12 and 8% Histodenz), and the tubes were spun at 55,000 rpm for 3 h at 4°C (200,000 g). Fractions of 180 µl were collected from the top of the tube. The two upper fractions were merged and boiled for 30 min in 0.2% SDS in PNGase F buffer (20 mM phosphate buffer pH 7.0, 25 mM EDTA, 0.6% NP-40, 1% β-mercaptoethanol). After cooling, Triton X-100 was added to a final concentration of 0.75%. Deglycosylation was performed with PNGase F (1 U/100 µl, 37°C, 16 h).

Supplementary information
Supplementary information available online at
http://jcs.biologists.org/lookup/doi/10.1242/jcs.186981.supplemental

References
Aguzzi, A. and Calella, A. M. (2009). Prions: protein aggregation and infectious diseases. Physiol. Rev. 89, 1105-1152.

Ashok, A. and Hegde, R. S. (2009). Selective processing and metabolism of disease-causing mutant prion proteins. PLoS Pathog. 5, e1000479.

Balch, W. E., Morimoto, R. I., Dillin, A. and Kelly, J. W. (2008). Adapting proteostasis for disease intervention. Science 319, 916-919.

Barik, S. (2006). Immunophilins: for the love of proteins. Cell. Mol. Life Sci. 63, 2889-2900.

Ben-Gedalya, T. and Cohen, E. (2012). Quality control compartments coming of age. Traffic 13, 635-642.

Ben-Gedalya, T., Lyakhovetsky, R., Yedidia, Y., Bejerano-Sagie, M., Kogan, N. M., Karpuj, M. V., Kaganovich, D. and Cohen, E. (2011). Cyclosporin-A-induced prion protein aggresomes are dynamic quality-control cellular compartments. J. Cell Sci. 124, 1891-1902.

Ben-Gedalya, T., Moll, L., Bejerano-Sagie, M., Frere, S., Cabral, W. A., Friedmann-Morvinski, D., Slutsky, I., Burstyn-Cohen, T., Marini, J. C. and Cohen, E. (2015). Alzheimer's disease-causing proline substitutions lead to presenilin 1 aggregation and malfunction. EMBO J. 34, 2820-2839.

Brodsky, R. A., Mukhina, G. L., Li, S., Nelson, K. L., Chiurazzi, P. L., Buckley, J. T. and Borowitz, M. J. (2000). Improved detection and characterization of paroxysmal nocturnal hemoglobinuria using fluorescent aerolysin. Am. J. Clin. Pathol. 114, 459-466.

Cabral, W. A., Perdivara, I., Weis, M., Terajima, M., Blissett, A. R., Chang, W., Perosky, J. E., Makareeva, E. N., Mertz, E. L., Leikin, S. et al. (2014). Abnormal type I collagen post-translational modification and crosslinking in a cyclophilin B KO mouse model of recessive osteogenesis imperfecta. PLoS Genet. 10, e1004465.

Cohen, E. and Taraboulos, A. (2003). Scrapie-like prion protein accumulates in aggresomes of cyclosporin A-treated cells. EMBO J. 22, 404-417.

Drisaldi, B., Stewart, R. S., Adles, C., Stewart, L. R., Quaglio, E., Biasini, E., Fioriti, L., Chiesa, R. and Harris, D. A. (2003). Mutant PrP is delayed in its exit from the endoplasmic reticulum, but neither wild-type nor mutant PrP undergoes retrotranslocation prior to proteasomal degradation. J. Biol. Chem. 278, 21732-21743.

Duennwald, M. L., Echeverria, A. and Shorter, J. (2012). Small heat shock proteins potentiate amyloid dissolution by protein disaggregases from yeast and humans. PLoS Biol. 10, e1001346.

Endo, T., Groth, D., Prusiner, S. B. and Kobata, A. (1989). Diversity of oligosaccharide structures linked to asparagines of the scrapie prion protein. Biochemistry 28, 8380-8388.

Helenius, A. and Aebi, M. (2004). Roles of N-linked glycans in the endoplasmic reticulum. Annu. Rev. Biochem. 73, 1019-1049.

Hessa, T., Sharma, A., Mariappan, M., Eshleman, H. D., Gutierrez, E. and Hegde, R. S. (2011). Protein targeting and degradation are coupled for elimination of mislocalized proteins. Nature 475, 394-397.

Hsiao, K., Baker, H. F., Crow, T. J., Poulter, M., Owen, F., Terwilliger, J. D., Westaway, D., Ott, J. and Prusiner, S. B. (1989). Linkage of a prion protein missense variant to Gerstmann-Sträussler syndrome. Nature 338, 342-345.

Jansen, C., Parchi, P., Capellari, S., Vermeij, A. J., Corrado, P., Baas, F., Strammiello, R., van Gool, W. A., van Swieten, J. C. and Rozemuller, A. J. (2010). Prion protein amyloidosis with divergent phenotype associated with two novel nonsense mutations in PRNP. Acta Neuropathol. 119, 189-197.

Johnston, J. A., Ward, C. L. and Kopito, R. R. (1998). Aggresomes: a cellular response to misfolded proteins. J. Cell Biol. 143, 1883-1898.

Junne, T., Wong, J., Studer, C., Aust, T., Bauer, B. W., Beibel, M., Bhullar, B., Bruccoleri, R., Eichenberger, J., Estoppey, D. et al. (2015). Decatransin, a new natural product inhibiting protein translocation at the Sec61/SecYEG translocon. J. Cell Sci. 128, 1217-1229.

Kim, S. J., Mitra, D., Salerno, J. R. and Hegde, R. S. (2002). Signal sequences control gating of the protein translocation channel in a substrate-specific manner. Dev. Cell 2, 207-217.

Kim, Y. E., Hipp, M. S., Bracher, A., Hayer-Hartl, M. and Hartl, F. U. (2013). Molecular chaperone functions in protein folding and proteostasis. Annu. Rev. Biochem. 82, 323-355.

Lawson, V. A., Collins, S. J., Masters, C. L. and Hill, A. F. (2005). Prion protein glycosylation. J. Neurochem. 93, 793-801.

Lisanti, M. P., Field, M. C., Caras, I. W., Menon, A. K. and Rodriguez-Boulan, E. (1991). Mannosamine, a novel inhibitor of glycosylphosphatidylinositol incorporation into proteins. EMBO J. 10, 1969-1977.

Merulla, J., Fasana, E., Soldà, T. and Molinari, M. (2013). Specificity and regulation of the endoplasmic reticulum-associated degradation machinery. Traffic 14, 767-777.

Misumi, Y., Miki, K., Takatsuki, A., Tamura, G. and Ikehara, Y. (1986). Novel blockade by brefeldin A of intracellular transport of secretory proteins in cultured rat hepatocytes. J. Biol. Chem. 261, 11398-11403.

Munro, S. and Pelham, H. R. B. (1987). A C-terminal signal prevents secretion of luminal ER proteins. Cell 48, 899-907.

Naslavsky, N., Stein, R., Yanai, A., Friedlander, G. and Taraboulos, A. (1997). Characterization of detergent-insoluble complexes containing the cellular prion protein and its scrapie isoform. J. Biol. Chem. 272, 6324-6331.

Noack, J., Brambilla Pisoni, G. and Molinari, M. (2014). Proteostasis: bad news and good news from the endoplasmic reticulum. Swiss. Med. Wkly. 144, w14001.

Obrig, T. G., Culp, W. J., McKeehan, W. L. and Hardesty, B. (1971). The mechanism by which cycloheximide and related glutarimide antibiotics inhibit peptide synthesis on reticulocyte ribosomes. J. Biol. Chem. 246, 174-181.

Oslowski, C. M. and Urano, F. (2011). Measuring ER stress and the unfolded protein response using mammalian tissue culture system. Methods Enzymol. 490, 71-92.

Prusiner, S. B. (1998). Prions. Proc. Natl. Acad. Sci. USA 95, 13363-13383.

Rane, N. S., Chakrabarti, O., Feigenbaum, L. and Hegde, R. S. (2010). Signal sequence insufficiency contributes to neurodegeneration caused by transmembrane prion protein. J. Cell Biol. 188, 515-526.

Ruggiano, A., Foresti, O. and Carvalho, P. (2014). Quality control: ER-associated degradation: Protein quality control and beyond. J. Cell Biol. 204, 869-879.

Schubert, U., Antón, L. C., Gibbs, J., Norbury, C. C., Yewdell, J. W. and Bennink, J. R. (2000). Rapid degradation of a large fraction of newly synthesized proteins by proteasomes. *Nature* **404**, 770-774.

Scott, M. R., Köhler, R., Foster, D. and Prusiner, S. B. (1992). Chimeric prion protein expression in cultured cells and transgenic mice. *Protein Sci.* **1**, 986-997.

Selkoe, D. J. (2003). Folding proteins in fatal ways. *Nature* **426**, 900-904.

Shaner, N. C., Campbell, R. E., Steinbach, P. A., Giepmans, B. N. G., Palmer, A. E. and Tsien, R. Y. (2004). Improved monomeric red, orange and yellow fluorescent proteins derived from Discosoma sp. red fluorescent protein. *Nat. Biotechnol.* **22**, 1567-1572.

Shao, J., Choe, V., Cheng, H., Tsai, Y. C., Weissman, A. M., Luo, S. and Rao, H. (2014). Ubiquitin ligase gp78 targets unglycosylated prion protein PrP for ubiquitylation and degradation. *PLoS ONE* **9**, e92290.

Soto, C. (2003). Unfolding the role of protein misfolding in neurodegenerative diseases. *Nat. Rev. Neurosci.* **4**, 49-60.

Stocki, P., Chapman, D. C., Beach, L. A. and Williams, D. B. (2014). Depletion of cyclophilins B and C leads to dysregulation of endoplasmic reticulum redox homeostasis. *J. Biol. Chem.* **289**, 23086-23096.

Suntharalingam, A., Abisambra, J. F., O'Leary, J. C., III, Koren, J., III, Zhang, B., Joe, M. K., Blair, L. J., Hill, S. E., Jinwal, U. K., Cockman, M. et al. (2012). Glucose-regulated protein 94 triage of mutant myocilin through endoplasmic reticulum-associated degradation subverts a more efficient autophagic clearance mechanism. *J. Biol. Chem.* **287**, 40661-40669.

Taraboulos, A., Raeber, A. J., Borchelt, D. R., Serban, D. and Prusiner, S. B. (1992). Synthesis and trafficking of prion proteins in cultured cells. *Mol. Biol. Cell* **3**, 851-863.

Taraboulos, A., Scott, M., Semenov, A., Avrahami, D., Laszlo, L. and Prusiner, S. B. (1995). Cholesterol depletion and modification of COOH-terminal targeting sequence of the prion protein inhibit formation of the scrapie isoform. *J. Cell Biol.* **129**, 121-132.

Torres, M., Medinas, D. B., Matamala, J. M., Woehlbier, U., Cornejo, V. H., Solda, T., Andreu, C., Rozas, P., Matus, S., Muñoz, N. et al. (2015). The protein-disulfide isomerase ERp57 regulates the steady-state levels of the prion protein. *J. Biol. Chem.* **290**, 23631-23645.

Walker, L. C., Levine, H., III, Mattson, M. P. and Jucker, M. (2006). Inducible proteopathies. *Trends Neurosci.* **29**, 438-443.

Winklhofer, K. F., Heller, U., Reintjes, A. and Tatzelt, J. (2003). Inhibition of complex glycosylation increases the formation of PrPsc. *Traffic* **4**, 313-322.

Xia, D., Tang, W. K. and Ye, Y. (2016). Structure and function of the AAA+ ATPase p97/Cdc48p. *Gene* **583**, 64-77.

Yamazaki, M., Oyanagi, K., Mori, O., Kitamura, S., Ohyama, M., Terashi, A., Kitamoto, T. and Katayama, Y. (1999). Variant Gerstmann-Sträussler syndrome with the P105L prion gene mutation: an unusual case with nigral degeneration and widespread neurofibrillary tangles. *Acta Neuropathol.* **98**, 506-511.

Yanai, A., Meiner, Z., Gahali, I., Gabizon, R. and Taraboulos, A. (1999). Subcellular trafficking abnormalities of a prion protein with a disrupted disulfide loop. *FEBS Lett.* **460**, 11-16.

Yang, W. and Storrie, B. (1998). Scattered Golgi elements during microtubule disruption are initially enriched in trans-Golgi proteins. *Mol. Biol. Cell* **9**, 191-207.

Yedidia, Y., Horonchik, L., Tzaban, S., Yanai, A. and Taraboulos, A. (2001). Proteasomes and ubiquitin are involved in the turnover of the wild-type prion protein. *EMBO J.* **20**, 5383-5391.